PROGRESS IN COLOR, COLORANTS AND COATINGS

available online @ www.pccc.icrc.ac.ir

Prog. Color Colorants Coat. 10 (2017), 205-216

Ministry of Science, Research and Technology
Institute for Color Science and Technology

Electrochemical Evaluation of Polyvinyl Butyral Coating Containing Polypyrrole/ZnO Nanocomposite for Corrosion protection of Al Alloy

G.S. Sajadi[1], S.M.A. Hosseini[1], M.J. Bahrami[2], M. Shahidi[*1,3]

[1.] Department of Chemistry, Shahid Bahonar University of Kerman, P.O. Box: 76169, Kerman, Iran.

[2.] Department of Science, Farhangian University, P. O. Box: 76166, Kerman, Iran.

[3.] Department of Chemistry, Kerman Branch, Islamic Azad University, P. O. Box: 7635131167, Kerman, Iran.

ARTICLE INFO

Article history:
Received: 06 Jul 2017
Final Revised: 20 Sept 2017
Accepted: 24 Sept 2017
Available online: 27 Sept 2017

Keywords:
Nanocomposite
Polyvinyl butyral
Electrochemical Impedance Spectroscopy
Electrochemical Noise
Wavelet Analysis.

ABSTRACT

In this work, polypyrrole/ZnO nanocomposite (PPy/ZnO NC) was produced through synthesis of polypyrrole polymer in the presence of ZnO nanoparticles. The corrosion behavior of polyvinyl butyral coatings without and with different weight percentages of nanocomposite on the surface of 7075 Al alloy was investigated in 3.5% NaCl solution at different immersion times using electrochemical impedance spectroscopy (EIS) and electrochemical noise (EN) techniques. The coating with 0.025% PPy/ZnO NC revealed the highest corrosion resistance. In order to analysis of EN data, wavelet transform was used to obtain the standard deviation of partial signal (SDPS) plots. The good agreement between the EIS and EN results indicates that the EN technique, as well as the EIS method, can be used successfully for the corrosion evaluation of coatings. Prog. Color Colorants Coat. 10 (2017), 205-216© Institute for Color Science and Technology.

1. Introduction

Aluminum and its alloys are widely used in many industries such as pipes, aerospace, machinery and chemical batteries [1]. The corrosion resistance of aluminum and its alloys arises from a rapidly formed, compact and strongly adherent oxide film on its surface [2, 3]. The oxide film is readily susceptible to corrosion in chloride environments [4].

Polymer coating on the metal surface is one of the most effective and economical techniques for corrosion protection [5-9]. Polyvinyl butyral (PVB) coating is usually used for applications that require strong binding, optical clarity, adhesion to many surfaces, toughness and flexibility. Polypyrrole (PPy) is among the group of conducting polymeric materials that have been used most widely because of its good electrical conductivity and environmental stability. In addition, PPy is readily synthesized using a range of aqueous and non-aqueous solvents [10]. Its technological applications in different areas such as electronic devices, sensors and corrosion protection are among the most active areas of research in polymer science and engineering [11].

It has been shown that the synthesis of polymers in the presence of nanoparticles (NPs) can increase the polymer surface area [12]. The incorporation of the conducting polymer as the shell in the core–shell structure can increase the surface area of the conducting polymers over that of the bulk polymer [11]. This structure can be obtained from an in situ

*Corresponding author: shahidi@iauk.ac.ir,
meshahidizandi@gmail.com

chemical oxidative polymerization in the presence of nanoparticles. The inorganic core can be a metal or a metal oxide, and the organic shell can be a conducting polymer.

Nanocomposite is a multiphase solid material in which one of the phases has one, two or three dimensions of less than 100 nm, or structures having nano-scale repeat distances between the different phases that make up the material. The mechanical, electrical, thermal, optical, electrochemical and catalytic properties of the nanocomposite will differ markedly from that of the individual components. In mechanical terms, nanocomposites differ from conventional composite materials due to the exceptionally high surface to volume ratio of the reinforcing phase and/or its exceptionally high aspect ratio.

Electrochemical noise (EN) is a promising technique for corrosion analysis which has gained popularity in the recent years [13-21]. EN measurements can be performed in freely corroding systems without the external application of electrical signals, so that the natural evolution of corrosion processes is assured. EN is defined as the fluctuations of potential or current originating from the corrosion events in a corrosion process. Two nominally identical working electrodes (WEs) are connected via a zero-resistance ammeter (ZRA) monitoring the coupling current between the electrodes.

While the EN measurement is simple, the understanding of the information included in the EN signals, i.e. the EN analysis, remains difficult. Wavelet transform is a data analysis procedure without the precondition of stationarity or linearity and with a high distinguishing capacity in both time and frequency domain simultaneously [17-20]. Wavelet transform describes the EN signal at several time scales in so-called crystals. The frequency range of each crystal is represented by the following equation [19]:

$$\left(f_1, f_2\right) = \left(2^{1-j} f_s \ , \ 2^{-j} f_s\right) \tag{1}$$

where f_s is sampling frequency, and j is the number of the crystal. The scale range of each crystal is given by the equation:

$$\left(I_1, I_2\right) = \left(2^{j-1}\Delta t \ , \ 2^{j}\Delta t\right) \tag{2}$$

where Δt is the sampling interval $\left(\Delta t = 1/f_s\right)$. Table 1 shows the frequency and scale range of the case in which $f_s = 4Hz$.

The inverse wavelet transform can produce partial signals of the original signal. Each partial signal is a signal which resembles the fluctuations of the original signal at a particular time scale. The standard deviation of partial signal (SDPS) can indicate the variations in the intensity of the partial signal about its mean, which could be an indication of the intensity of electrochemical activity on the surface of the electrodes within a particular interval of frequency [19].

Table 1: Frequency and scale range of each crystal for the case of $f_s = 4Hz$.

Crystal name	Frequency range/Hz	Scale range/s
d1	4-2	0.25-0.5
d2	2-1	0.5-1
d3	1-0.5	1-2
d4	0.5-0.25	2-4
d5	0.25-0.125	4-8
d6	0.125-0.0625	8-16
d7	0.0625-0.0312	16-32
d8	0.0312-0.0156	32-64

The plot of the SDPS versus their corresponding crystal name is called SDPS plot. Such a plot provides mechanistic information about physical processes: the position of the maximum in the SDPS plot indicates the dominant process in certain corrosion events and its change can reflect the behavior of the dominant corrosion process. For a more detailed discussion on wavelet transform and SDPS plot, one can refer to an earlier paper [19].

In this paper, the corrosion behavior of polyvinyl butyral coatings with different concentrations of polypyrrole/ZnO nanocomposite (PPy/ZnO NC) on the surface of 7075 Al alloy was investigated in 3.5% NaCl solution using electrochemical impedance spectroscopy (EIS) and electrochemical noise (EN) techniques.

2. Experimental

2.1. Materials

Pyrrole, methyl orange (MO), chloroferric, sodium chloride, zinc nitrate, zinc oxide, sodium hydroxide, methanol and polyvinyl butyral (PVB) were purchased from Merck. All chemicals were used without any further purification. The employed working electrodes were prepared from 7075 aluminum alloy with the chemical composition (wt.%) of: Zn (5.91), Mg (2.42), Cu (1.83) and Fe (0.26).

2.2. Methods

ZnO nanoparticles (ZnO NPs) were prepared according to the previously reported procedure [22]. The solutions of 0.45 M zinc nitrate ($Zn(NO_3)_2.4H_2O$) and 0.9 M sodium hydroxide (NaOH) were prepared in distilled water. Then, the beaker containing NaOH solution was heated at the temperature of about 55 ºC. The zinc nitrate solution was added drop wise (slowly for 40 min) to the above heated solution under high speed stirring. The beaker was sealed at this condition for 2h. The precipitated ZnO NPs were cleaned with deionized water and ethanol then dried in air atmosphere at about 60 ºC. The final product was white powder.

PPy/ZnO NC was prepared by in situ chemical oxidation [11]. At first, 0.58 g $FeCl_3$ was dissolved in 5 mM MO. Then, 0.19 g ZnO NP was dispersed in the mixture by magnetic stirring for 30 min. After that, 0.2 mL pyrrole monomer was slowly added to the solution. The polymerization was performed under static conditions for 24 h at 0–5 °C. The precipitate was filtered and washed repeatedly with distilled water then dried in a vacuum oven at 50 °C for 36 h.

For preparation of coatings, 2-g sample of 60,000 MW polyvinyl butyral (PVB) was dissolved in 20 mL methanol with continuous stirring for 24 h. The PPy/ZnONC powder was introduced to the PVB solution under continuous stirring for 24 h. Various coatings containing 0, 0.0125, 0.025 and 0.05 wt% of PPy/ZnONC were prepared. The coating without PPy/ZnONC (0% NC) was used as blank.

The specimens were connected to a copper wire at one end, and then sealed using epoxy resin with the other end exposed as the working electrode (WE). Before coating application, the WE surface was abraded by wet abrasive papers through 600–2500 grade, washed with distilled water, degreased with acetone and finally dried in air. Clean working electrodes were coated by dip-coating. The withdrawing rate was 18 cm/min and the immersion time in the PVB with and without PPy/ZnONC was 100 s.

EIS and EN experiments were conducted using Autolab 302 N potentiostat equipped with Nova 1.6 software. EIS measurements were conducted in a conventional three-electrode cell. A platinum rod and a saturated (KCl) Ag/AgCl electrode were used as the counter and reference electrodes, respectively. The working electrode was a coated 7075 Al alloy with a surface area of 100 mm^2. A sinusoidal potential perturbation of 10 mV versus OCP was used in the EIS measurements and a frequency range from 10 mHz to 100 kHz was employed. The impedance data were analyzed with Nova software.

Two WEs were facing each other vertically at a distance of about 2 cm in the EN experiments. An identical uncoated WE was used as the second WE. The entire cell was placed inside a Faraday cage to limit external electromagnetic interference. The sampling frequency for the electrochemical noise data was 4 Hz. Noise data were analyzed with wavelet technique using the orthogonal Daubechies wavelets of the fourth order (db4). The necessary calculations for construction of the SDPS plots were performed using Matlab software. Samples were analyzed using Scanning electron microscopy (SEM) and X-Ray diffraction (XRD).

3. Results and discussion

The SEM image of PPy/ZnO NPs in Figure 1 shows that a bulk quantity of flower-like bunches exist. Each bunch is gathered of closely packed nanometer scale rods. Figure 2 also shows the SEM images of PPy/ZnO NC. As seen from Figure 1 and Figure 2, the ZnO NPs and PPy/ZnO NC are approximately in the range of 30-70 nm. Figure 3 shows the XRD images of PPy/ZnO NC. All the peaks correspond to the reflections of PPy/ZnO NC (Peak List) which are in good accordance with standard diffraction data of ZnO (JCPDS card no. 80-0075).

3.1. Electrochemical impedance spectroscopy

Figure 4 shows the Bode plots of the coatings containing different concentrations of PPy/ZnO NC at various times after immersion in 3.5% NaCl solution. The curves in Figure 4 clearly show that the impedance increases with increasing the concentration of NC up to 0.025 wt%.

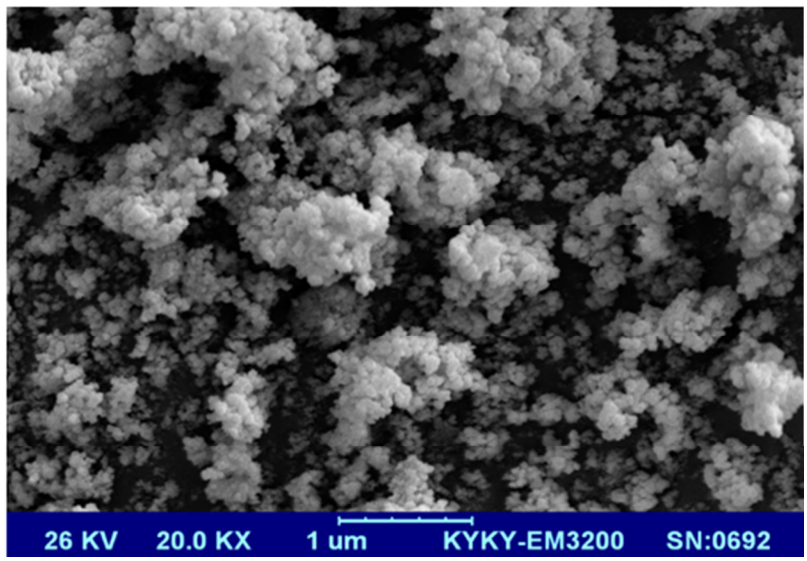

Figure 1: SEM images of PPy/ZnO NPs.

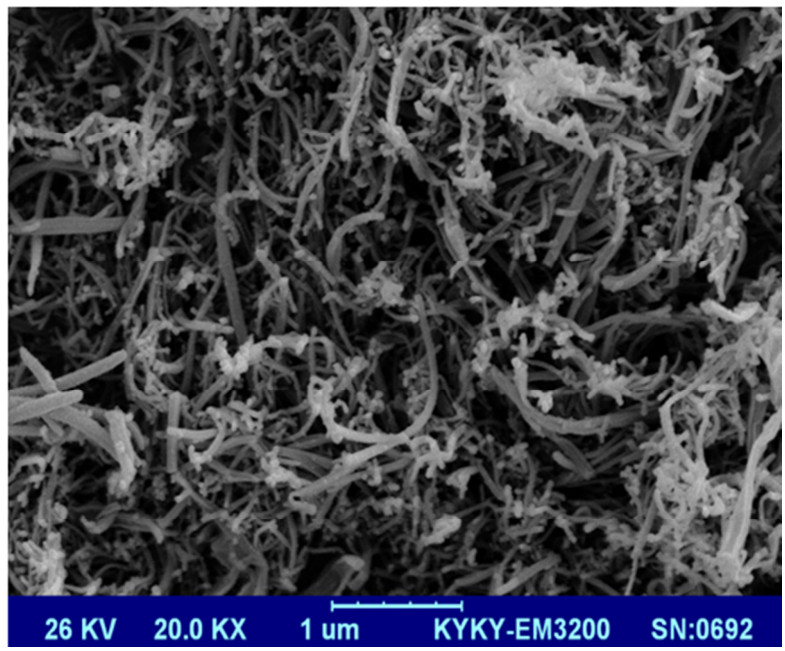

Figure 2: SEM images of PPy/ZnO NC.

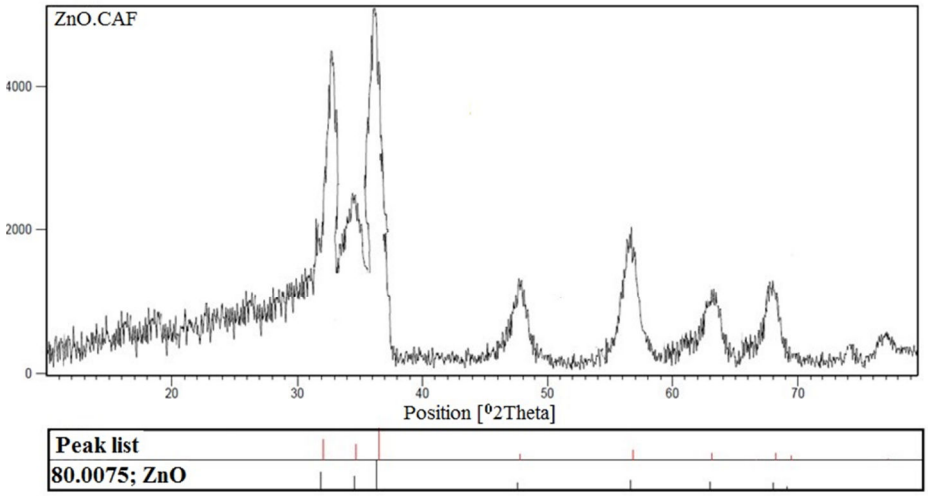

Figure 3: XRD images of PPy/ZnO NC.

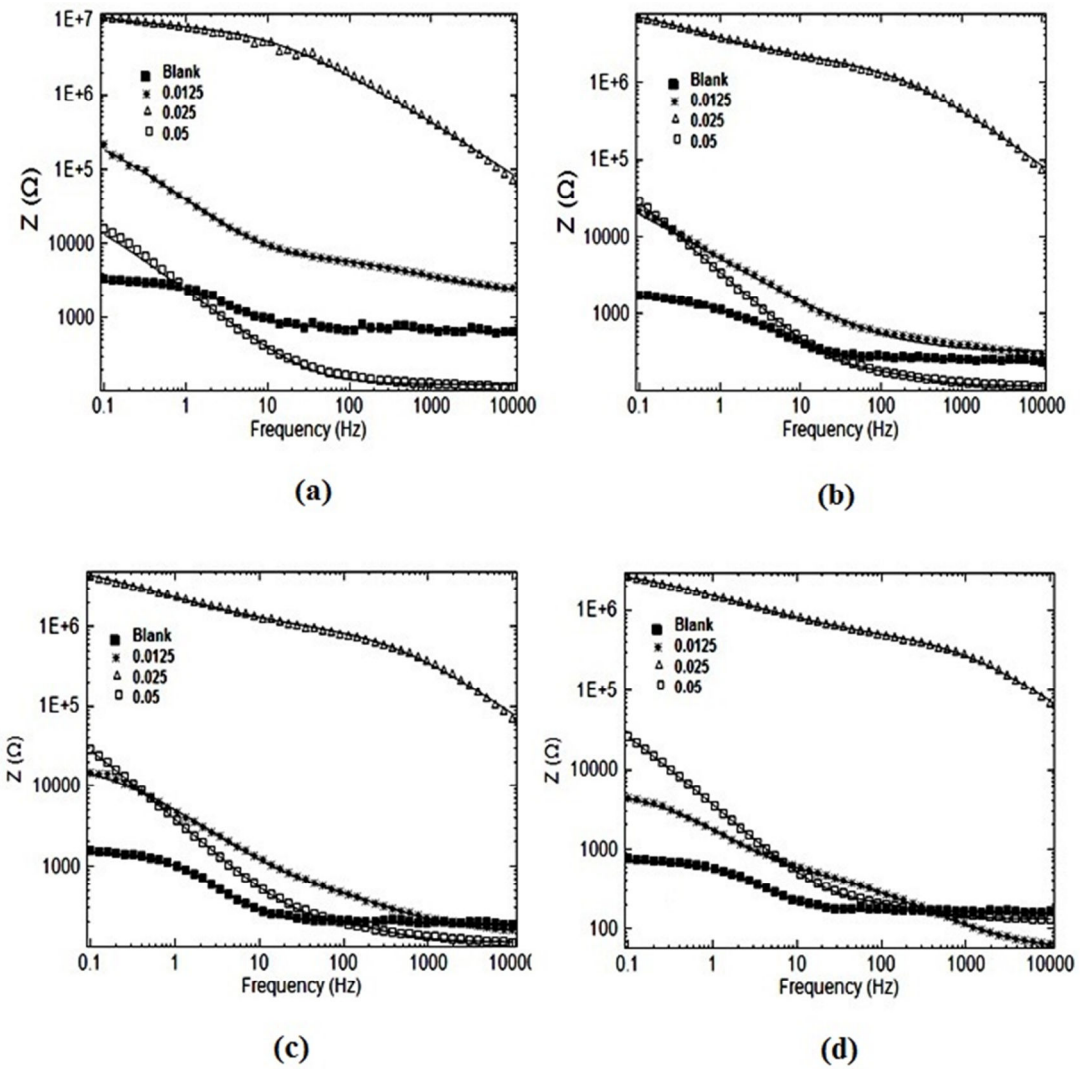

Figure 4: Bode plots of various coatings in the absence and presence of different concentrations of PPy/ZnO NC and immersed in 3.5% NaCl solution for (a) 6 day, (b) 16 day, (c) 26 day and (d) 36 day.

Figure 5 shows the equivalent electrical circuit employed to analyze the impedance plots. This circuit is composed of two time constants in cascade, accounting for coating capacitance and pore resistance (Q_c/R_{po}) and double layer and surface corrosion effects (Q_{dl}/R_{ct}). Table 2 lists the impedance parameters of various coated samples with and without PPy/ZnO NC. As it can be seen from Table 2, for all immersion times, the R_{ct} values increase as the concentration of PPy/ZnO NC increases up to 0.025 wt%. Protection efficiencies in Table 2 were calculated through the following expression:

$$PE(\%) = \frac{R_{ct}^{'} - R_{ct}}{R_{ct}^{'}} \times 100 \quad (3)$$

where $R_{ct}^{'}$ and R_{ct} are the charge transfer resistances of the coating matrix with and without Nanocomposite, respectively. According to PE values in Table 2 it can be deduced that the concentration of 0.025 wt% exhibited the best performance for corrosion protection of Al Alloy.

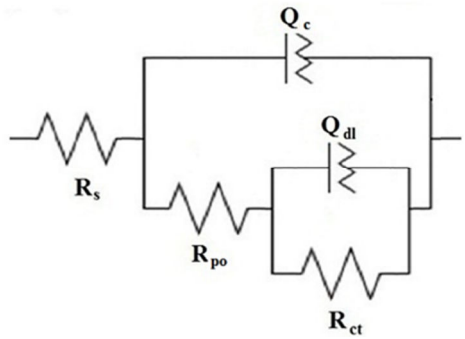

Figure 5: Equivalent Electrical circuit.

Table 2: The EIS parameters of various coatings in the absence and presence of different concentrations of PPy/ZnO NCs.

t_{imm}	Coat	R_{po}/kΩ.cm^2	R_{ct}/kΩ.cm^2	PE (%)
6 day	Blank	0.127	2.55	-
	0.0125	5.3	420	91.33
	0.025	9000	50000	99.99
	0.05	0.4	26	91.5
16 day	Blank	0.07	2.04	-
	0.0125	0.367	100	97.96
	0.025	2000	10000	99.97
	0.05	0.129	156	98.69
26 day	Blank	0.167	1.63	-
	0.0125	0.643	20.4	92
	0.025	1000	8000	99.97
	0.05	0.14	137	98.81
36 day	Blank	0.109	0.728	-
	0.0125	0.608	4.95	85.29
	0.025	500	3500	99.97
	0.05	0.143	84.2	99.13

3.2. Electrochemical noise

Figure 6 shows the EN signals corresponding to the coatings containing different concentrations of PPy/ZnO NC after various immersion times. Then wavelet analysis was employed to decompose each set of data points and then the SDPS plots of signals in Figure 6 were obtained as shown in Figure 7.

It is suitable to use the standard deviation of partial signal (SDPS) for calculation of the amount of noise charges at the particular frequency interval. The maximum peak in SDPS plots corresponds to predominant transients in the original EN signal [19]. However, it should be verified using the original EN signal that this maximum peak arises from the single transients rather than the overlapped transients. Comparison between partial and original signals provides another way of recognizing the scale of the predominant transients [23].

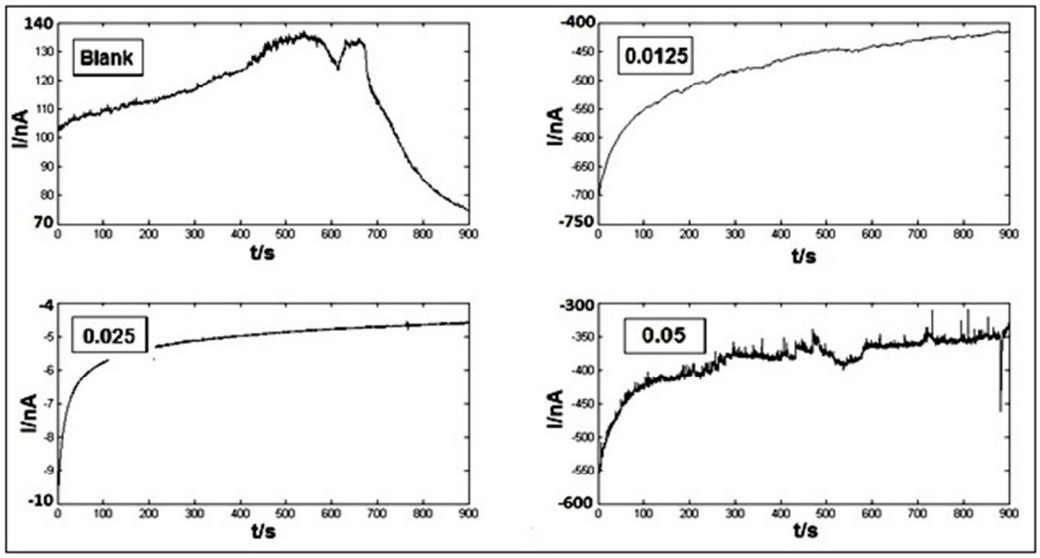

(a)

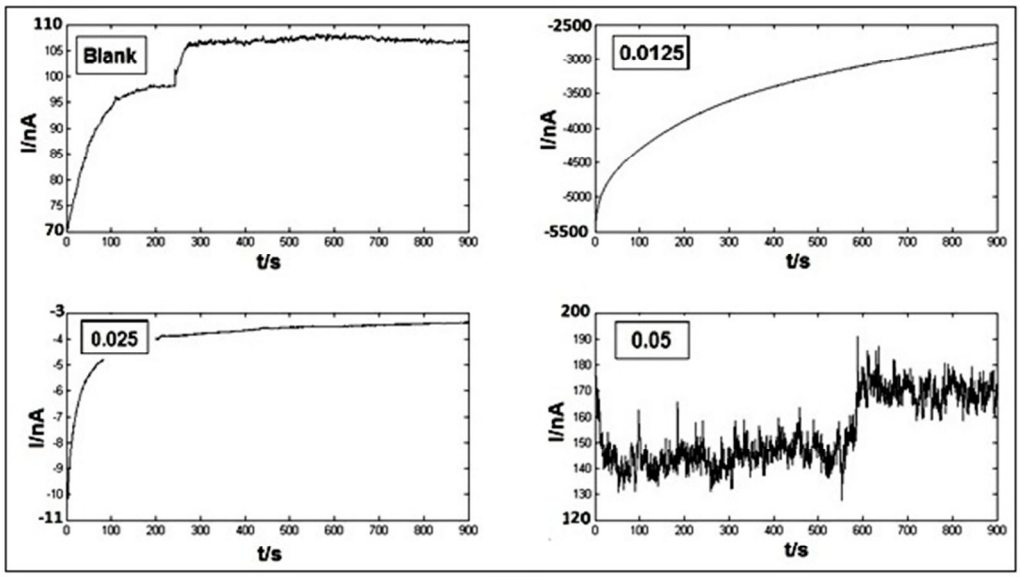

(b)

Figure 6: EN current records of various coatings in the absence and presence of different concentrations of PPy/ZnO NC and immersed in 3.5% NaCl solution for (a) 6 days, (b) 16 days, (c) 26 days and (d) 36 days.

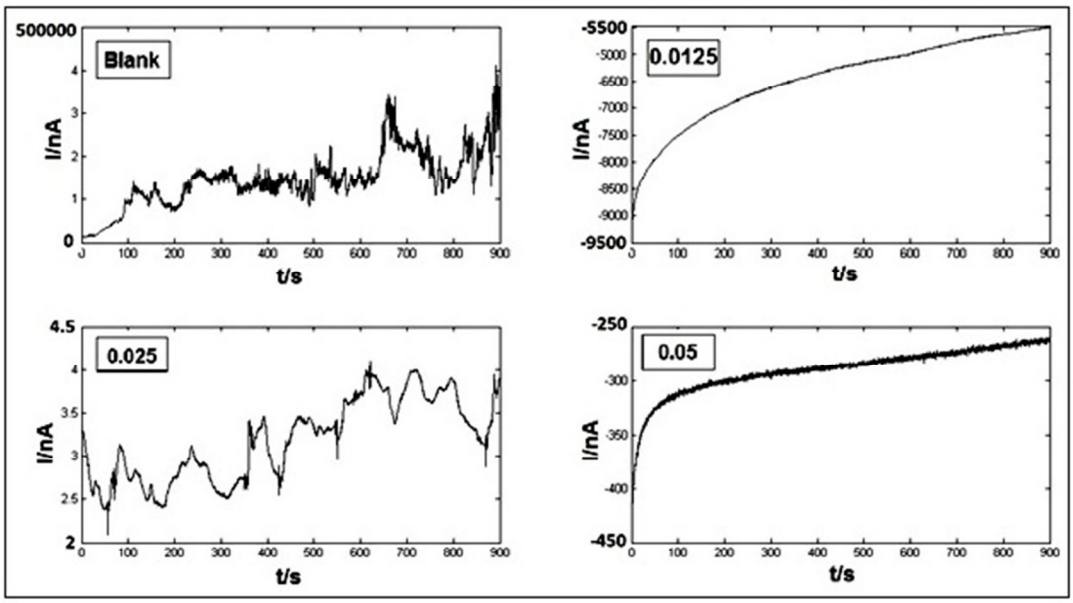

(c)

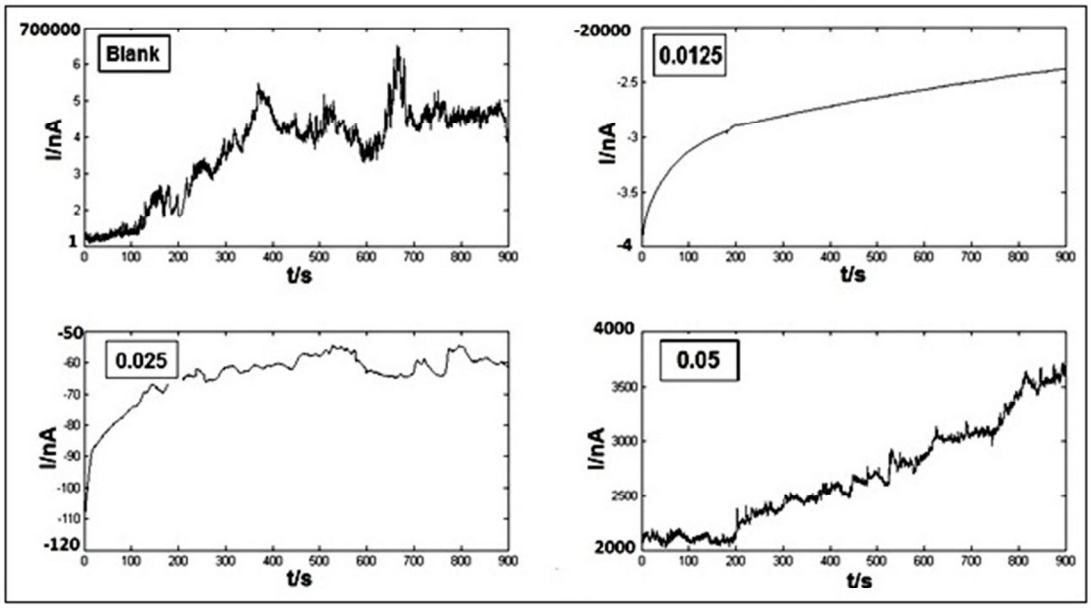

(d)

Figure 6: Continue.

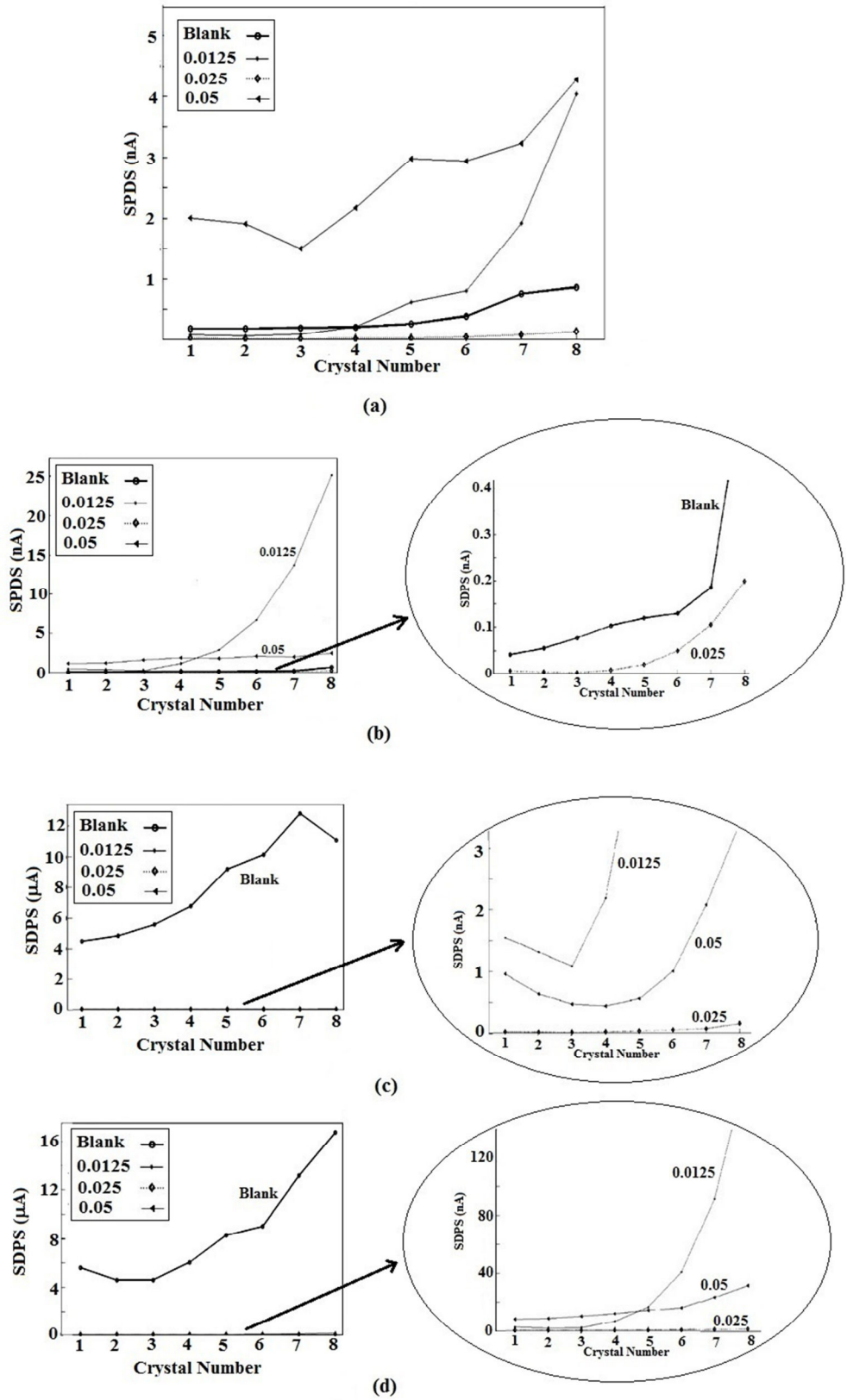

Figure 7: SDPS plot of signals in Figure 6.

Table 3: The EN parameters of various coatings in the absence and presence of different concentrations of of PPy/ZnO NCs.

t_{imm}	Coat	d_{max}	τ_{max}/s	$SDPS_{max}$/nA	Q/nCoul	PE(%)
6 day	Blank	d7	24	0.76	7.76	-
	0.0125	d4	3	0.2	0.6	92.26
	0.025	d1	0.375	0.001	0.00037	99.99
	0.05	d5	6	2.98	17.88	-
16 day	Blank	d8	48	0.64	8.64	-
	0.0125	d4	3	1.2	3.6	58.33
	0.025	d1	0.375	0.007	0.0026	99.96
	0.05	d4	3	1.85	5.55	35.76
26 day	Blank	d7	24	12800	307200	-
	0.0125	d4	3	4.8	14.8	99.99
	0.025	d1	0.375	0.14	0.025	99.99
	0.05	d6	12	1	12	99.99
36 day	Blank	d7	24	13400	341600	-
	0.0125	d5	6	19	114	99.96
	0.025	d4	3	0.1	0/3	99.99
	0.05	d5	6	12	72	99.97

The predominant transients can be attributed to metastable pits. The development of a pit causes a quantity of electric charge to flow in the circuit which can be estimated by the following equation (4) [8]:

$$Q = SDPS_{max}.\tau_{max} \quad (4)$$

where $SDPS_{max}$ is the SDPS value at the maximum peak crystal (d_{max}) and τ_{max} is the average time width of d_{max} crystal. Then it seems suitable to define the protection efficiencies as follows:

$$PE(\%) = \frac{Q - Q'}{Q} \times 100 \quad (5)$$

where Q and Q' are the noise charges of the coating matrix without (i.e. blank) and with NC, respectively.

The values of the parameters derived from all of the SDPS plots in Figure 7 have been summarized in Table 3. This table further presents values of PE. Comparison with data in Table 2 reveals that reasonable agreement is found with the PE values as obtained through EIS measurements. Again, concentration of 0.025 wt% exhibited the best performance to protect against corrosion.

4. Conclusions

The results obviously confirmed the synthesis of ZnONPs and PPy/ZnO NC. The diameter of the synthesized PPy/ZnO NC is in the range of 30-70 nm. After applying the epoxy coatings containing PPy/ZnO NC on Al alloy, the protection efficiency was investigated in 3.5% NaCl solution by EIS and EN methods. For all immersion times, the protection efficiency increases as the concentration of ZnO increases up to 0.025 wt%. However, the protection

efficiency values decreased with increasing the immersion time.

It seems that the EN method can be applied as a complementary quantitative technique to study the corrosion behavior of coatings. According to the calculation of the amount of noise charges using the standard deviation of partial signal at the particular frequency interval, it was possible to obtain the protection efficiency of a coating. The protection efficiencies obtained from EN data showed a reasonable agreement with those obtained from EIS measurements.

Acknowledgements

This work has received financial support from Islamic Azad University, Kerman Branch.

5. References

1. E.A. Noor, Evaluation of inhibitive action of some quaternary N-heterocyclic compounds on the corrosion of Al–Cu alloy in hydrochloric acid, *Mater. Chem. Phys.*, 114(2009), 533-541.
2. Q. Zhang, Y. Hua, Corrosion inhibition of aluminum in hydrochloric acid solution by alkylimidazolium ionic liquids, *Mater. Chem. Phys.*, 119(2010), 57-64.
3. M. Shahidi, R.F. Moghaddam, M.R. Gholamhosseinzadeh, S.M.A. Hosseini, Investigation of the cathodic process influence on the electrochemical noise signals arising from pitting corrosion of Al alloys using wavelet analysis, *J. Electroanal. Chem.*, 693(2013), 114-121.
4. P.M. Natishan, W.E. O'Grady, Chloride Ion Interactions with Oxide-Covered Aluminum Leading to Pitting Corrosion: A Review, *J. Electrochem. Soc.*, 161(2014), C421-C432.
5. F. Mansfeld, Use of electrochemical impedance spectroscopy for the study of corrosion protection by polymer coatings, *J. Appl. Electrochem.*, 25(1995), 187-202.
6. Z. Ranjbar, S. Ashhari, A. Jannesari, S. Montazeri, Effects of Nano Silica on the Anticorrosive Properties of Epoxy Coatings, *Prog. Color Colorants Coat.*, 6(2013), 119-128.
7. M. Rashvand, Z. Ranjbar, Cathodic Electrodeposion of Nanotitania along with the Epoxy Based Coating and Evaluation of its Anticorrosion Properties, *Prog. Color Colorants Coat.*, 7(2014), 227-235.
8. M. Hasanzadeh, M. Shahidi, M. Kazemipour, Application of EIS and EN techniques to investigate the self-healing ability of coatings based on microcapsules filled with linseed oil and CeO_2 nanoparticles, *Prog. Org. Coat.*, 80(2015), 106-119.
9. A. Golgoon, M. Aliofkhazraei, M.Toorani, A.R.S. Rouhaghdam, Corrosion Protection Performance of Nanoclay-Polyester Nanocomposite Coatings, *Prog. Color Colorants Coat.*, 9(2016), 223-232.
10. M.R. Mahmoudian, W.J. Basirun, Y. Alias, Synthesis of polypyrrole/Ni-doped TiO_2 nanocomposites (NCs) as a protective pigment in organic coating, *Prog. Org. Coat.*, 71(2011), 56-64.
11. M.R. Mahmoudian, Y. Alias, W.J. Basirun, M. Ebadi, Effects of different polypyrrole/TiO_2 nanocomposite morphologies in polyvinyl butyral coatings for preventing the corrosion of mild steel, *Appl. Surf. Sci.*, 268(2013), 302-311.
12. M.R. Mahmoudian, W.J. Basirun, Y. Alias, A.K. Zak, Electrochemical characteristics of coated steel with poly(N-methyl pyrrole) synthesized in presence of ZnO nanoparticles, *Thin Solid Films*, 520(2011), 258-265.
13. Y. Tan, Sensing localised corrosion by means of electrochemical noise detection and analysis, *Sensor Actuat. B-Chem.* , 139(2009), 688-698.
14. R.A. Cottis, Interpretation of Electrochemical Noise Data, *Corrosion*, 57(2001), 265-285.
15. G. Schmitt, K. Moeller, P. Plagemann, Online monitoring of crevice corrosion with electrochemical noise, *Mater. Corros.*, 55(2004), 742-747.
16. G. Schmitt, Listen to corrosion at work - A newly developed versatile corrosion monitoring tool ready for plant application, *Mater. Corros.*, 58(2007), 924-939.
17. A. Aballe, M. Bethencourt, F.J. Botana, M. Marcos, Using wavelets transform in the analysis of electrochemical noise data, *Electrochim. Acta*, 44(1999), 4805-4816.
18. M.T. Smith, D.D. Macdonald, Wavelet Analysis of Electrochemical Noise Data, *Corrosion*, 65(2009), 438-448.
19. M. Shahidi, S.M.A. Hosseini, A.H. Jafari, Comparison between ED and SDPS plots as the results of wavelet transform for analyzing electrochemical noise data, *Electrochim. Acta*, 56(2011), 9986-9997.
20. A.M. Homborg, T. Tinga, X. Zhang, E.P.M.v. Westing, P.J. Oonincx, G.M. Ferrari, J.H.W.d. Wit, J.M.C. Mol, Transient analysis through Hilbert spectra of electrochemical noise signals for the identification of localized corrosion of stainless steel, *Electrochim. Acta*, 104(2013), 84-93.
21. A. Mohammadi, S.M.A. Hosseini, M.J. Bahrami, M. Shahidi, Corrosion Inhibition of Mild Steel in Acidic

Solution by Apricot Gum as a Green Inhibitor, *Prog. Color Colorants Coat.*, 9(2016), 117-134.
22. A.B. Moghaddam, T. Nazari, J. Badraghi, M. Kazemzad, Synthesis of ZnO Nanoparticles and Electrodeposition of Polypyrrole/ZnO Nanocomposite Film, *Int. J. Electrochem. Sci.*, 4(2009), 247-257.
23. M. Shahidi, A.H. Jafari, S.M.A. Hosseini, Comparison of Symmetrical and Asymmetrical Cells by Statistical and Wavelet Analysis of Electrochemical Noise Data, *Corrosion*, 68(2012), 1003-1014.

How to cite this article:
G.S. Sajadi, S.M.A. Hosseini, M.J. Bahrami, M. Shahidi, Electrochemical Evaluation of Polyvinyl Butyral Coating Containing Polypyrrole/ZnO Nanocomposite for Corrosion protection of Al Alloy. Prog. Color Colorants Coat., 10 (2017), 205-216.